 ation information: DOI 10.1109/TPWRS.2018.2829079, IEEE

Power System Reliability Evaluation Incorporating Dynamic Thermal Rating and Network Topology Optimization

Ruosong Xiao, *Student Member, IEEE*, Yingmeng Xiang, *Student Member, IEEE*, Lingfeng Wang, *Senior Member, IEEE*, and Kaigui Xie, *Senior Member, IEEE*

***Abstract*—The electrical power grid is a critical infrastructure that plays a key role in supporting modern society. The reliability of power systems needs to be continuously maintained to deliver high-quality electric services. Due to the tremendous amounts of potential investment demanded for constructing new electricity transmission facilities, electric utilities need economical solutions that can enable them to supply electricity to their customers in a cost-effective and reliable way. Dynamic thermal rating (DTR) and network topology optimization (NTO) technologies aim to maximize the use of existing transmission assets and to provide flexible ways to enhance reliability of the power system. In this study, the DTR and NTO are incorporated into the power grid reliability assessment procedure using the sequential Monte Carlo simulation. Multiple case studies are carried out based on the modified IEEE RTS-79 and IEEE RTS-96 systems, accounting for long-term multi-area weather conditions. The numerical results indicate that with the incorporation of DTR and NTO, the reliability of power systems can be improved. The effect of these methods is especially significant for power grids with lower electricity delivery capabilities.**

***Index Terms*—Dynamic thermal rating, network topology optimization, reliability improvement, operational strategies.**

NOMENCLATURE

1) Indices

b	Index for the substations.
d	Index for the load demands.
e	$e \in \{fr, to\}$. Index for the {from, to} end of the transmission lines.
g	Index for the generators.
i	Index for the busbars. $i \in \{1, 2\}$.
l	Index for the lines.

2) Sets

G_b/D_b	Set of the generators/loads in substation b.
$LF_b/\ LT_b$	Set of the transmission lines whose directions of power flow are from/to substation b.

3) Parameters

δ^{max}	Maximum allowed voltage angle.
M_l	A sufficiently great number.
P_d^{max}	Maximal amount of load demand d.
P_g^{min}/P_g^{max}	Lower/upper bound of power output of generator g.
P_l^{max}	Transmission capacity limit of the line l.
n_b^{max}/n_l^{max}	Maximum number of allowed busbar switching/line switching actions.
n_s^{max}	Maximum allowed number of total switching actions.
x_l	Impedance of the line l.

4) Variables

$\delta_{b,i}$	Angle of the voltage at busbar i in substation b.
$\delta_{l,e}$	Angle of the voltage of transmission line l at end e.
$\delta_{l,e,i}$	Angle of the voltage at busbar i associated with end e of transmission line l.
h_b	Binary variable determining the connection of the two busbars in substation b (0: disconnected, 1: connected).
h_l	Binary variable determining the switching state of the transmission line l (0: open, 1: closed).
$h_d/h_g/h_{l,e}$	Binary variable determining which one of the two busbars the load /generator/ end e of transmission line l is connected to.
I	Conductor ampacity (rating).
mC_p	Conductor's total heat capacity.
$P_{d,i}/P_{g,i}$	Load demand/generation output connected to busbar i

This work was supported in part by the National Science Foundation (NSF) under Award ECCS1711617, and in part by the National Natural Science Foundation of China under Award 51377178.

R. Xiao was with the Department of Electrical Engineering and Computer Science, University of Wisconsin-Milwaukee, Milwaukee, WI 53211, USA and the State Key Laboratory of Power Transmission Equipment & System Security, School of Electrical Engineering, Chongqing University, Chongqing 400030, China. He is now with the State Grid Chengdu Gaoxin Power Supply Company, Chengdu 610041, China.

Y. Xiang is with Global Energy Interconnection Research Institute (GEIRI) North America, San Jose, CA 95134, USA.

L. Wang is with the Department of Electrical Engineering and Computer Science, University of Wisconsin-Milwaukee, Milwaukee, WI 53211, USA (email: l.f.wang@ieee.org) (*Corresponding author: Lingfeng Wang*).

K. Xie is with the State Key Laboratory of Power Transmission Equipment & System Security, School of Electrical Engineering, Chongqing University, Chongqing 400044, China.

 ation information: DOI 10.1109/TPWRS.2018.2829079, IEEE

P_l	Power flow on line l.
$P_{l,e,i}$	Line power flow on line l of which the end e is connected to busbar i.
Q_c	Rate of convection heat loss.
Q_r	Rate of radiated heat loss.
Q_s	Rate of solar heat gain.
$R(T_c)$	Conductor AC resistance at the temperature T_c.
T_a	Ambient temperature.
T_c	Critical conductor temperature.

I. Introduction

Reliability is one of the most important requirements for electrical power systems. In recent years, various kinds of smart grid technologies are proposed, developed and deployed in the power systems, such as renewable generations, microgrids, and cutting-edge communication and control methods. It is becoming more and more challenging for electric utilities to ensure the reliability of power systems in the face of emerging uncertainties. Thus, the impacts of these technologies on power system reliability need to be carefully examined, which has spurred high interests on the related topics. For example, in [1] the high penetration of wind power on the reliability evaluation of power systems is studied. Also, the power system reliability is evaluated considering other types of renewable generation such as tidal generation [2] and solar generation [3].

For all kinds of technologies, their impacts on the power system reliability are heavily dependent on their associated operation strategies. The integration of FACTS devices [4], [5] and energy storage [6] could increase the flexibility of power system operations in normal and contingency states, which is beneficial to enhancing the power system reliability. Yet these technologies usually require tremendous amounts of investment. Meanwhile, although the smart grid technologies can increase the power system reliability, they bring cyber risks. The increasing dependence of the power system on the associated cyber layer for monitoring and control inevitably brings vulnerabilities for cyber intrusions and hacking. This could increase the occurrence probability of the cyber-induced failures, and lead to the power system reliability degradation. Some research has been performed investigating the impacts of cyberattack risks on power system reliability such as [7] and authors' previous work [8].

Clearly, some considerations should be given to those technologies which explore the potential of existing power system assets and improve the system reliability in a cost-effective manner. In this spirit, this paper is then focused on improving the power system reliability efficiently. Two representative cost-effective methods are considered: the dynamic thermal rating (DTR) [9] and the network topology optimization (NTO) [10]. The dynamic thermal rating can increase the transmission capacity without extra investments for building new lines; the network topology optimization is a novel power system operation strategy, which can potentially minimize the load shedding in the face of a contingency. Furthermore, as two representative cost-effective methods, they can work jointly to further increase the power system reliability.

Traditionally, transmission line ratings are determined based on the static thermal rating (STR) method, which calculates line ratings with assumed conservative weather conditions and may result in possible underestimations of transmission line ratings [11]. Differently, the DTR method accounts for the real-time, variable environmental conditions which may thus release the underestimated transmission capacities. Various field tests have been conducted to quantify the capacity increment that DTR is able to bring to OHLs. It has been reported that by enforcing DTR, in over 96% of the time the line rating could be increased; the increment itself may vary from 5% to 50%, or even over 150% in some specific conditions; the overall network transmission capacity has also been reported to be probably increased by 15% [12], [13]. With the ability to boost the network transmission capacity, DTR is very suitable to be integrated into system operations for fulfilling particular operating objectives. In [14] DTR has been incorporated into a power system economic dispatch to reduce either the generation cost or the transmission lost. In [15] a real-time congestion management problem considering DTR is discussed. The effect of the enforcement of DTR into a security constrained unit commitment problem is presented in [16]. Meanwhile, due to the correlation between DTR and the wind power generation, studies have also indicated the specific benefits that DTR brings to wind generation integrated power systems [17]. The impacts of the DTR on the power system reliability have also attracted much attention. It has been proved that the deployment of DTR will improve the power system reliability [18], [19]. In addition, by coordinating DTR with other smart grid technologies, the potential benefit may be more dramatic. As shown in [20], DTR is deployed with an optimal demand response scheme for an improved performance. And in [21], DTR is adopted along with the optimal transmission switching mechanism to enhance the system reliability.

Similar to DTR, network topology control is a type of technology that helps to optimize the system operation by adjusting the transmission network configuration in contrast with traditional fixed topology based optimal power dispatch. Switching the transmission lines on/off is one of the common ways to change the network topology. This optimal transmission switching mechanism (OTS) has been envisioned in [22] and modeled as a mixed integer linear programming (MILP) problem as an extension to traditional DC-OPF (shortly denoted as "OPF" in the rest of this paper) in [23]. Later, OTS has been proposed for realizing different operating goals in various studies. In [24], OTS is enforced to reduce the system total cost/loss. Reference [25] presents the deployment of OTS for reducing costs as well as satisfying the N-1 reliability standard. Moreover, in [26] the impact of OTS on the unit commitment problem is discussed. Another approach to adjust the network topology is the reconfiguration of high voltage substations. Theoretically, since generators, load demands, transmission lines and substation busbars are all connected through switching devices (e.g., circuit breakers), the operation of these switching devices (such as busbar switching) will

 ation information: DOI 10.1109/TPWRS.2018.2829079, IEEE

generate different configurations of component connections and result in different network topologies. It has been demonstrated in [27], [28] that the busbar switching (BBS) can improve the short-term power system operation security, such as preventing transmission overloading and reducing load curtailment. Then in [10] a novel system topology optimization technology is proposed that considers the optimal switching of both transmission lines and busbars, namely, the NTO. It is shown in [10] that with the added busbar switching mechanism, NTO could equip the power system with a higher operating flexibility. Also, it has been demonstrated in [10] that with the incorporation of NTO the operating congestion can be dramatically relieved and the operating cost can then be significantly reduced. This novel technology has also attracted considerable attention more recently due to its promising capability of better using the existing power delivery infrastructure.

Both DTR and NTO share a common intrinsic philosophy, i.e., they both increase the system's power delivery capability through relaxing some conventional operating constraints and without the need of building new power transfer facilities. It is thus a natural thought that the incorporation of both technologies into power system operating strategies would improve the power system reliability in a cost-effective manner. This research aims to incorporate DTR and NTO into the conventional reliability assessment framework of power systems and to quantify the impact of these new operating strategies on the power system reliability, especially for complex, large-scale power systems accounting for influence of long-term, multi-area weather conditions.

The major contributions of this paper are summarized as follows:

(1) We propose to jointly use multiple cost-effective methods to maximize the power system reliability. The DTR and NTO, as two promising cost-effective methods, are integrated into the power system reliability evaluation model. The joint evaluation of such cost-effective methods, to the authors' best knowledge, are novel or have not been emphasized in the existing literature.

(2) The long-term multi-area weather conditions in a bulk power system are considered in the DTR model, which enables a more comprehensive and practical DTR model as compared with the existing work.

(3) The NTO method is integrated into the power system reliability evaluation model with efficient computational burden reduction technique in the Monte Carlo simulation. The advantage of NTO over the traditional OPF, OTS, and BBS are demonstrated with comparative case studies.

In summary, this paper is significantly different from the existing work, as we propose to jointly adopt multiple cost-effective methods based on different mechanisms to improve the power system reliability efficiently and economically, while considering the practical and computational issues of the methods.

The organization of this paper is laid out as follows: The DTR models are discussed in section II; the NTO modeling is described in section III; the power grid reliability evaluation procedure incorporating DTR-NTO is proposed in section IV; section V describes the simulation studies and presents the case study outcomes; and section VI summarizes this study and provides future research directions.

II. Overhead Line Dynamic Thermal Rating

From both system planning and operation perspectives, transmission line ratings are critical quantities for electrical power transmission networks. Inadequate transmission line ratings may become weak links within the transmission system, limiting the total power transfer capability and compromising the overall system reliability [29], [30]. Therefore, more accurate line rating estimation methods become highly necessary. Dynamic line rating is such a technology by considering that the overhead lines (OHLs) rating is practically influenced by a variety of real-time factors. There are several ways to determine OHL dynamic line ratings, such as weather monitoring based methods, conductor temperature monitoring based methods, conductor sag measuring/clearance monitoring based methods, conductor tension measuring based methods, and so forth [31]. Among these methods, DTR accounts for the varying operating conditions and calculates the OHL ratings according to the conductor's thermal behaviors.

With the consideration of varying operating conditions, DTR could produce more accurate OHL rating estimations. However, in actuality there is no guarantee that the enforcement of DTR could always bring benefits to power systems. For critical infrastructures such as electrical power systems, where the reliability and security are among the top priorities in both their planning and operation activities, implementing DTR could be risky in certain situations. The possible drawbacks of DTR come first from its high demand on the detailed, high-resolution weather data. The erroneous data, either the false real-time monitoring data or the erroneous forecasted data, could degrade the estimation accuracy and result in biased assessments of DTR performance [32]. Additionally, DTR is highly dependent on the weather conditions. The performance of DTR may vary for different locations of different climatic types. Hence, neglecting the climatic and geographical distributions could also lead to biased assessments of DTR performances [33]. However, even with the above drawbacks, the potential advantages of DTR are undoubtedly more prominent. Reference [34] has demonstrated that to achieve the same level of transmission capacity increase, DTR is much cheaper than the traditional network reinforcement solutions. Presently, DTR is recommended as a cost-effective strategy to utilize the power system assets more efficiently [35].

The mechanism of DTR has been discussed since 1970's [36]. Thus far, several standards are available for DTR calculations in practice, such as IEEE Standard 738 [37], IEC/TR 61597 [38], and CIGRE Technical Brochure 601 [39]. Generally, these methods take into account the surrounding conditions (e.g., velocity and direction of wind, solar radiation, environmental temperature, etc.) and calculate OHL real-time thermal ratings considering the conductor HBE (heat-balance equation). The heat-balance of power conductor is formed as the balance between conductor cooling (convection heat loss, radiative heat loss, evaporative cooling, etc.) and the conductor heating (solar

 ation information: DOI 10.1109/TPWRS.2018.2829079, IEEE

radiation heat gain, conductor Joule heat gain, skin effect heat gain, etc.) [40]. Difference between conductor heating and cooling will cause the changing of conductor temperature during the transient process, and eventually the heat loss rate along with the heat gain rate should match each other in a steady state manner. With real time monitored environment parameters and conductor parameters, the conductor ampacity, i.e., the OHL real time thermal rating can then be calculated through HBE. Although developed by different organizations, these calculation methods function in a similar way and offer ampacity estimations with only a small difference [41], [42]. Since it is often accepted that the IEEE Standard 738 is the most common method to obtain OHL thermal ratings in the U.S. [43], the DTR calculation in this study will follow the HBE form developed in such a standard.

In IEEE Standard 738, the HBE takes into account the convection and radiative heat losses, as well as the heat gain due to solar radiation and the conductor's Joule heat. A non-steady-state form of HBE is represented as follows:

$$Q_c(T_a, T_c, v_w) + Q_r(T_a, T_c) + mC_p\frac{dT_c}{dt} = Q_s + I^2R(T_c) \quad (1)$$

$$\frac{dT_c}{dt} = \frac{[Q_s + I^2R(T_c) - (Q_c(T_a, T_c, v_w) + Q_r(T_a, T_c))]}{mC_p} \quad (2)$$

These two differential equations indicate that the rates of the conductors' temperature would grow rapidly with the increase of the current in the conductor for the non-steady-state. Typically, for Drake aluminum cable steel reinforced (ACSR), the conductor temperature can reach a steady value within sufficient time, usually one hour [37]. In such a case, the conductor heat balance can be described as the steady-state HBE as follows:

$$Q_c(T_a, T_c, v_w) + Q_r(T_a, T_c) = Q_s + I^2R(T_c) \quad (3)$$

Therefore, the thermal rating of an OHL can be obtained as:

$$I = \sqrt{\frac{Q_c(T_a, T_c, v_w) + Q_r(T_a, T_c) - Q_s}{R(T_c)}} \quad (4)$$

Although the transient form of HBE such as (1) and (2) may derive the OHL dynamic thermal rating more accurately, the difference introduced by assuming a steady-state will not be significant especially if the transient process last for over 30 minutes, according to [43], [44]. For simplicity, the DTR model will follow the steady-state form HBE shown in (4) in this study.

The HBE expressed in (4) also indicates the fact that dynamic thermal line ratings are sensitive to the related weather conditions. Note these weather conditions are not only time-varying, but also geographically dispersed. Fig. 1 illustrates an example where some OHLs connecting bus A and B span across multiple geographical areas with different weather conditions. Intuitively, the windy section II and the rainy section IV may be in suitable weather conditions, for which the OHLs could achieve a capacity boost with DTR enforcement. Yet for safety considerations, the ratings should be determined by the most limiting span, i.e., the span under the harshest weather condition within the whole OHL [15]. Therefore, in this example, it is likely the whole OHL rating should be limited by the sunny section I. Ignorance of such consideration could result in a false estimation of OHL dynamic thermal ratings, and expose the line to risk of possible overloading conditions.

Some studies have been conducted to analyze the impact relating to the meteorological condition variations. For example, in [33] to achieve a more comprehensive DTR scheme, the weather condition variations have been considered in the DTR implementation. Also in [45] the ambient temperature variation is incorporated into the transmission line modeling. Furthermore, the impact brought about by the meteorological condition variation is investigated in [46] through various power flow analyses. Although these studies have pointed out the importance of considering weather condition variations, the previous studies on DTR-enforced power system analyses mostly neglected various meteorological impacts on transmission lines – they generally adopted relevant parameters' mean values for the whole area instead. Thus, it is necessary to more accurately study the reliability impacts of meteorological condition variations on DTR-enforced power systems. In this study, such impacts are taken into consideration in determining the final OHL rating for each transmission line which may span multiple areas with different weather conditions. The ultimate rating for a specific transmission line is the smallest value of all DTR outcomes calculated based on different weather conditions in different areas that the transmission line spans.

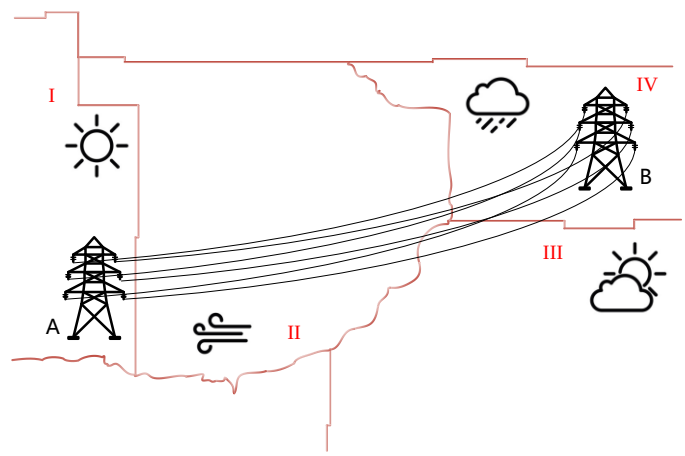

Fig. 1. An example of OHLs influenced by multi-area weather conditions

III. Network Topology Optimization Modeling

The substations play critical roles in the power grid, as they are the junction points for power flows, generation outputs, and load demands. The substations are made up of multiple devices for performing the needed functions such as power transformation and metering. These elements can be connected to or disconnected from the substation by controlling the related switching devices, especially the circuit breakers. The number of circuit breakers as well as their connections to the busbars are of great importance, as they could influence the power delivery reliability, the power system operation flexibility, and even the security of the substations. There are various kinds of bus system with respect to different configurations of circuit breakers and busbars in the bulk power system. Due to the high reliability and flexibility performance, it is often suggested to implement a breaker and a half arrangement in high-voltage

 ation information: DOI 10.1109/TPWRS.2018.2829079, IEEE

substations [47], as illustrated in Fig. 2.

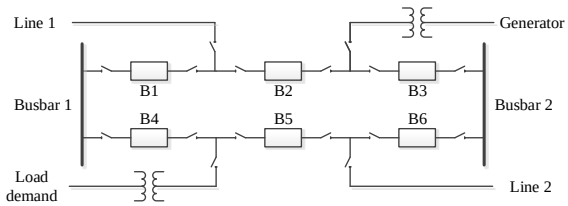

Fig. 2. Schematic of breaker and a half bus system

Assuming the breaker and a half bus system is pervasively adopted in the power grid, a generalized NTO model can be shown in Fig. 3. The switching actions involved in the NTO model are illustrated as follows as well. It also indicates the great flexibility that the system could benefit from the NTO mechanism: with different switching configurations, the busbars of the two buses and the transmission line can be in either a connected/close state or a separated/open state; the generators, load demands and transmission line ends can be switched to either of the two busbars, respectively.

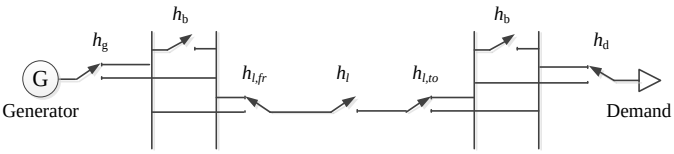

Fig. 3. Generalized model for network topology optimization

The switching actions can be represented with binary variables. Here, a binary variable h_b is used to determine the connection state of the busbars; a binary variable h_l is used to determine the switching state of the transmission line; and binary variables h_g, h_d and $h_{l,e}$ are used to identify which of the two busbar the generator, load demand and the line has been connected to.

Then, the NTO model is mathematically formulated in detail by the following equations/constraints [10]. For two busbars in a same substation, their voltage angles are identical if they are connected, otherwise independent, as described by (5):

$$-\delta^{max}(1-h_b) \le \left(\delta_{b,1}-\delta_{b,2}\right) \le \delta^{max}(1-h_b)\ \forall b \quad (5)$$

Constraints (6)-(7) describes the generator output limits, and their connection to either one of the two busbars in the related substation.

$$\left(1-h_g\right)P_g^{min} \le P_{g,1} \le \left(1-h_g\right)P_g^{max}\ \forall g \quad (6)$$

$$h_g P_g^{min} \le P_{g,2} \le h_g P_g^{max}\ \forall g \quad (7)$$

Similarly, constraints (8)-(9) indicate a load demand in a substation can connect to either one of the two busbars in the related substation. In addition, constraints (8)-(9) also consider possible load curtailment, as the actual load demands can be less than the maximum load demand.

$$0 \le P_{d,1} \le (1-h_d)P_d^{max}\ \forall d \quad (8)$$

$$0 \le P_{d,2} \le h_d P_d^{max}\ \forall d \quad (9)$$

The relationships and constraints related to transmission lines are mathematically represented by (10)-(14).

$$-\left(1-h_{l,e}\right)P_l^{max} \le P_{l,e,1} \le \left(1-h_{l,e}\right)P_l^{max}\ \forall l,e \quad (10)$$

$$-h_{l,e}P_l^{max} \le P_{l,e,2} \le h_{l,e}P_l^{max}\ \forall l,e \quad (11)$$

$$-h_l P_l^{max} \le P_{l,e,1} \le h_l P_l^{max}\ \forall l,e \quad (12)$$

$$h_{l,e} \le h_l\ \forall l,e \quad (13)$$

$$P_l = P_{l,fr,1} + P_{l,fr,2}\ \forall l \quad (14)$$

Constraints (10) and (11) represent the switching options at the line ends; constraints (12) and (13) describe the service status on the line; the power flow at the end of the line is calculated considering the possible power flows from the two busbars in (14).

The line power flow is described in constraints (15)-(17).

$$-(1-h_l)M_l \le \frac{\delta_{l,fr}-\delta_{l,to}}{x_l} - P_l \le (1-h_l)M_l\ \forall l \quad (15)$$

$$-h_{l,e}\delta^{max} \le \delta_{l,e}-\delta_{l,e,1} \le h_{l,e}\delta^{max}\ \forall l \quad (16)$$

$$-(1-h_{l,e})\delta^{max} \le \delta_{l,e}-\delta_{l,e,2} \le (1-h_{l,e})\delta^{max}\ \forall l,e \quad (17)$$

Considering that if the busbars are interconnected, there will be no need to differentiate which busbar the generator, load demand, or line end are connected to. Constraints (18)-(20) are thus introduced to tighten the constraints.

$$h_b + h_g \le 1\ \forall b\ g \in G_b \quad (18)$$

$$h_b + h_d \le 1\ \forall b\ d \in D_b \quad (19)$$

$$h_b + h_{l,e} \le 1\ \forall b,e\ l \in LF_b\ or\ l \in LT_b \quad (20)$$

The balance between the power entering and the power leaving a busbar is denoted by (21)-(22)

$$\sum_{g\in G_b} P_{g,1} - \sum_{d\in D_b} P_{d,1} - \sum_{l\in LF_b} P_l + \sum_{l\in LT_b} P_l = 0\ \forall b \quad (21)$$

$$\sum_{g\in G_b} P_{g,2} - \sum_{d\in D_b} P_{d,2} - \sum_{l\in LF_b} P_l + \sum_{l\in LT_b} P_l = 0\ \forall b \quad (22)$$

Limitations of the maximal number of allowable switching actions are described by (23)-(25). In practice, if the values of n_b^{max}, n_l^{max} and n_s^{max} are sufficiently large, all switching actions would be considered simultaneously.

$$\sum_{b=1}^{n_b}(1-h_b) \le n_b^{max} \quad (23)$$

$$\sum_{l=1}^{n_l}(1-h_l) \le n_l^{max} \quad (24)$$

$$\sum_{l=1}^{n_l}(1-h_l) + \sum_{b=1}^{n_b}(1-h_b) \le n_s^{max} \quad (25)$$

In reliability analysis, the main concern is to minimize the amount of the possible load curtailment, i.e., maximally satisfy the load demands. Thus, the objective function for the NTO problem formulation applied to reliability analysis is shown in (26).

$$\max \sum_{d=1}^{n_d}(P_{d,1}+P_{d,2}) \quad (26)$$

The whole NTO problem formulation consists of (5)-(26). The mathematical model forms an MILP optimization problem. Such a problem can be solved by commercial solvers such as CPLEX [48]. Note in this NTO problem formulation, if n_b^{max} is set to be zero, i.e., no busbars are allowed to split, the NTO problem becomes an OTS problem; if n_l^{max} is set to be zero, i.e., no transmission lines are allowed to switch, the NTO problem becomes a BBS problem; and if both n_b^{max} and n_l^{max} are set to be zero, the problem returns to the original OPF problem form. Again, it should be noted that the term "OPF" used in this paper represents the traditional DC-OPF widely used in power system reliability evaluation.

Table I lists the comparison among OPF, OTS, BBS, and NTO models used in reliability evaluation. With the ability to reconfigure connections of transmission lines, generators, loads, and busbars, NTO combines both the OTS and BBS mechanisms. It can be seen from this table that, from the mathematical modeling point of view, the OPF, OTS and BBS problems are in fact specific forms of the NTO problem: they all share the same objective function; yet by removing some constraints, the NTO problem could be transformed to either

 ation information: DOI 10.1109/TPWRS.2018.2829079, IEEE

TABLE I
COMPARISON OF OPF, OTS, BBS AND NTO MODELING USED IN RELIABILITY EVALUATION

Model		OPF	OTS	BBS	NTO
Object function		Minimizing system total load curtailment	Minimizing system total load curtailment	Minimizing system total load curtailment	Minimizing system total load curtailment
Decision variables	Continuous variables	Generator outputs, nodal load curtailments	Generator outputs, nodal load curtailments	Generator outputs, nodal load curtailments	Generator outputs, nodal load curtailments
	Binary variables	-	Switching states of transmission lines	Connection states of substation busbars; Connection statuses of generators, loads and transmission line ends	Switching states of transmission lines; Connection states of substation busbars; Connection statuses of generators, loads and transmission line ends
Constraints		Bus voltage angle limits	Bus voltage angle limits	Bus/busbar voltage angle limits	Bus/busbar voltage angle limits
		Generator output limits	Generator output limits	Generator output limits	Generator output limits
		Branch transmission capacity limits	Branch transmission capacity limits	Branch transmission capacity limits	Branch transmission capacity limits
		Nodal load curtailment limits	Nodal load curtailment limits	Nodal/busbar load curtailment limits	Nodal/busbar load curtailment limits
		Power balance equation at each bus	Power balance equation at each bus	Power balance equation at each bus/busbar	Power balance equation at each bus/busbar
		DC power flow equation of each branch	DC power flow equation of each branch, considering the transmission line switching states	DC power flow equation of each branch	DC power flow equation of each branch, considering the transmission line switching states
			Limit of allowable switchable transmission lines	Limits of allowable switchable substation busbars	Limit of allowable switchable transmission lines
					Limits of allowable switchable substation busbars
Problem formulations		LP	MILP	MILP	MILP

OTS, BBS or OPF problem. As addressed in [10], NTO is able to provide the system with a higher flexibility and lead to a reduced operating cost as compared to either OTS, BBS or OPF. Similarly, it can be concluded here that, as a comprehensive optimal control strategy for transmission network topology, NTO could help find the relatively more optimized network topology switching scheme, based on which the total load curtailment could be minimized. And for practical system operations, the NTO technology could make the fullest use of existing transmission facilities and provide the system operator with a higher flexibility on network topology control. In summary, the presented NTO model could enable improved system flexibility with respect to both OTS and BBS, and consequently will further enhance the system reliability.

IV. INCORPORATING DTR-NTO INTO RELIABILITY EVALUATION FRAMEWORK

Since both the DTR and NTO technology possess the ability to boost the transmission capacity, it is prospective that the enforcement of both DTR and NTO could improve the overall power system reliability as well. In addition, when compared to the case that only NTO is enforced through system operating, since mostly the OHL dynamic thermal rating would be higher than the static thermal rating, the DTR-NTO incorporation may help release system congestion conditions. The NTO model may find possible better reconfiguration solutions then. On the other hand, when compared to the case that only DTR is considered, as the NTO mechanism possess the ability to adjust network topology, load curtailment in some system operating state may be reduced, or even avoided. Thus undoubtedly, the reliability improvement would be maximized when DTR and NTO are enforced simultaneously.

To demonstrate such a reliability improvement, a DTR-NTO incorporated reliability evaluation framework is proposed in this study based on the sequential Monte Carlo simulation (MCS). In general, the sequential MCS-based reliability evaluation framework includes several basic steps. The component reliability models should be established first. With the component reliability related parameters coupled with the network conformation data, random system states are sampled by using the sequential MCS. Load curtailments for all sampled states will be calculated through the optimal power flow (OPF) analysis. Finally, after sampling sufficient amounts of system states, with all the sampled states as well as the corresponding load curtailment records, reliability indices representing power supply adequacy from differing angles can be calculated.

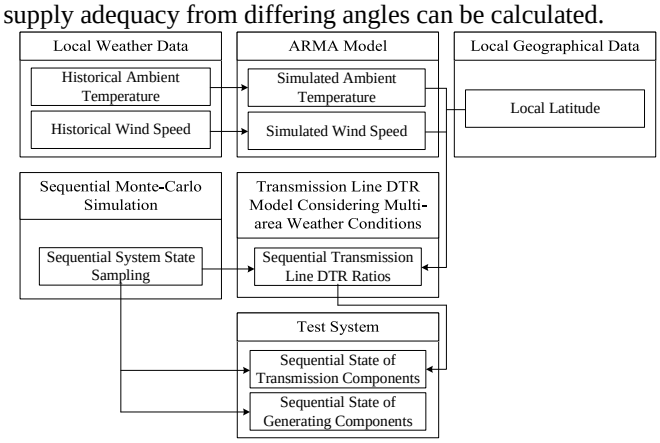

Fig. 4. Flowchart of DTR in reliability evaluation procedure incorporating DTR-NTO

 ation information: DOI 10.1109/TPWRS.2018.2829079, IEEE

With the incorporation of the DTR mechanism, transmission line ratings will be determined dynamically with corresponding environmental changes. Since DTR requires detailed weather information which is usually not easy to obtain for a long-term period, here an ARMA (Auto-Regressive and Moving Average) model is adopted to generate sufficient weather data. Meanwhile, note that the commonly used IEEE RTS does not offer detailed OHL information, which is required for the DTR calculation [24]. In this study, the modification of dynamic line ratings will be conducted through DTR ratios: for each hourly sampled system state, based on real-time weather data in each geographical area, local DTR ratios are first calculated as the ratios between the dynamic thermal line ratings and the static thermal line ratings. For long-distance OHLs crossing multiple areas, the overall DTR ratios will be determined according to different weather conditions within these areas: the lowest local DTR ratio among all crossed areas will be adopted as the final DTR ratio result for such OHLs. Finally, the OHL dynamic thermal ratings are determined through multiplying the DTR ratio with their original ratings, and the system data will be thus updated accordingly. The data flow chart of the above DTR processing in DTR-NTO incorporated reliability evaluation procedure is shown in Fig. 4.

NTO is essentially a system operation strategy, and the enforcement of NTO could reduce load curtailments of certain system states. Similar to OPF, in the DTR-NTO-based reliability evaluation procedure, the NTO model is used to calculate system load curtailments of sampled states in MCS. It should be noted here that to save the computational cost, in scenarios where load demands for all customers are already satisfied, or the system load curtailment calculated by OPF is zero, the NTO procedure will not be executed. Otherwise, it will be executed. The resultant load curtailment along with the performance of NTO will be recorded for further analysis.

The flowchart of the overall DTR-NTO-based reliability evaluation procedure is depicted in Fig. 5.

V. Simulation Studies

To demonstrate the influence of the integration of DTR-NTO, IEEE RTS-79 [42] and IEEE RTS-96 [43] with appropriate modifications are adopted as the test systems. All OHLs are assumed to be standard 795 kcmil 26/7 overhead bare Drake ACSR conductors. The normal operating climatic condition for static thermal rating calculation is assumed with an environmental temperature of 40 °C, a full-sun condition and a wind velocity of 0.61m/s. The maximum allowable conductor surface temperature is assumed to be 100 °C, and the wind direction is assumed to remain perpendicular to OHLs.

Weather data to be used are first obtained from the NOAA (National Oceanic and Atmospheric Administration) daily and hourly climate Normals dataset of 13 stations located in the state of Wisconsin [51]. Table II gives a brief look at the locations, ambient temperatures, wind speeds and latitudes of these stations. An ARMA model is then adopted to generate sufficient hourly weather data points required for performing sequential MCS.

As mentioned before, in practice, electrical power systems are large-scale, interconnected networks operating in complex environments. Hence, to show the impact of multi-area dynamic weather states on the enforcement of DTR-NTO, the test systems are assumed to be geographically divided into different areas and then sectionalized with respect to different stations: the RTS-79 test system is sectionalized into four areas (Section I-IV) and the RTS-96 is sectionalized into 13 different areas (Section I-XIII), as shown in Fig. 6 and Fig. 8, respectively. Then for comparing the performance of different operation strategies integrations, simulations are conducted for these following cases:

a. Basic OPF enforced.
b. NTO enforced.
c. DTR and OPF enforced.
d. DTR and NTO enforced.

TABLE II
Weather Data of 13 Locations in Wisconsin

Section	Location	Temperature Range (°C)	Wind Speed Range (m/s)	Latitude
I	Milwaukee	-21.16-34.12	0-12.52	42.955°N
II	Green Bay	-23.17-34.78	0-12.20	44.4794°N
III	Madison	-22.13-34.70	0-9.68	43.1406°N
IV	La Crosse	-25.23-36.59	0-13.10	43.8792°N
V	Kenosha	-21.76-34.72	0-14.69	42.595°N
VI	Sheboygan	-22.89-34.21	0-12.10	43.7694°N
VII	Racine	-21.25-34.12	0-11.50	42.7611°N
VIII	Oshkosh	-23.15-34.77	0-11.33	43.9844°N
IX	Eau Claire	-27.42-34.89	0-11.04	44.8653°N
X	Alexander Field	-24.62-34.21	0-9.80	44.3592°N
XI	Fond du Lac	-23.15-34.78	0-12.60	43.77°N
XII	Wausau ASOS	-25.87-34.17	0-12.50	44.9286°N
XIII	Lone Rock Tri	-23.75-33.60	0-13.10	43.2119°N

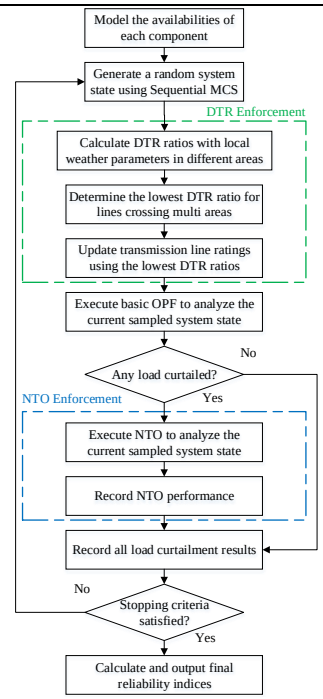

Fig. 5. Flow chart of DTR-NTO incorporated reliability evaluation procedure

For brevity, these test scenarios are denoted as "OPF," "NTO," "DTR-OPF," and "DTR-NTO" in the following discussions, respectively. The time period used in the sequential

ation information: DOI 10.1109/TPWRS.2018.2829079, IEEE

MCS is specified to be 50 years so that the coefficient of variation for EDNS can be guaranteed to be not more than 2%. The simulation environment for this study is based on MATLAB, and IBM CPLEX is used to solve the NTO problem.

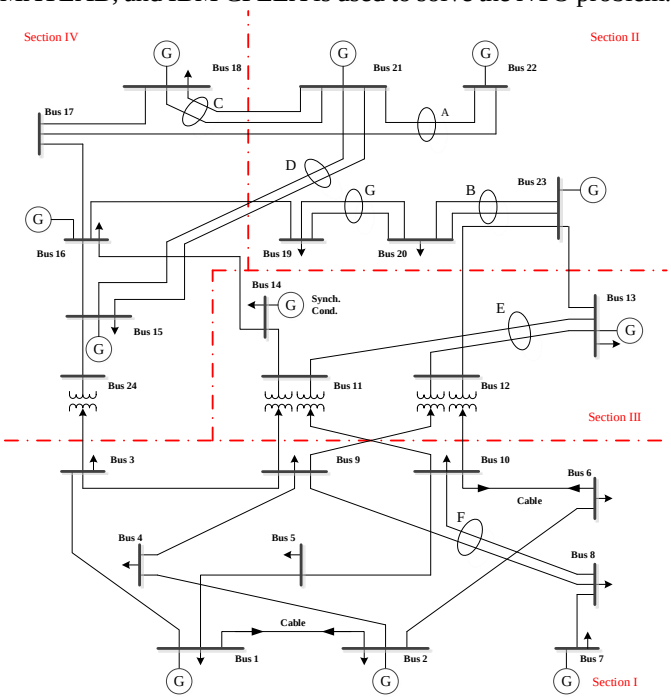

Fig. 6. Sectionalized RTS-79 system reflecting multi-area weather conditions

A. Impact of Multi-Area Weather Conditions on DTR Enforcement

Simulations are first conducted on the sectionalized IEEE RTS-79 system to demonstrate how multi-area weather conditions will affect the system reliability when DTR is enforced. The original ratings of all OHLs in the system has been modified to be 60% of their original values in [49].

Fig. 7 demonstrates part of the hourly dynamic thermal rating calculations with the consideration of multi-area weather conditions. The result contains the increments of hourly dynamic line ratings brought by the DTR mechanism in 2 weeks, within section III, section IV, and of the whole OHL connecting bus 14 and bus 16, crossing sections III and IV. Clearly, the quite dissimilar climatic characteristics in sections III and IV have induced volatile DTR increments. For lines crossing different areas, as the example OHL line 23, demonstrated in Fig. 7, it is thus important to properly determine the dynamic line ratings. Without considering multi-area weather conditions, the dynamic line ratings could be either overestimated or underestimated. Meanwhile, the results indicate that the OHL DTR increments presented in Fig. 7 may not be positive in some rare cases. At these moments, due to the harsh weather condition, the dynamic line rating is in fact lower than its static thermal rating value. However, as discussed previously the advantage of DTR is still more prominent: as the results in Fig. 7 have revealed, the line rating would be improved in most time.

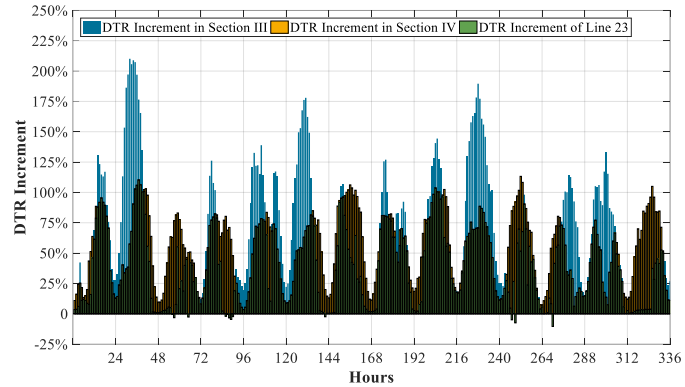

Fig. 7. An example of DTR calculation considering multi-area weather conditions

In addition, the system-level impacts of the multi-area weather conditions on DTR enforced system reliability are illustrated in Table III. The results indicate that with the enforcement of DTR, the system reliability level has been improved: compared to the basic OPF case, the LOLE index has dropped by 27.65%, the EENS index has dropped by 28.44%. In addition, by neglecting the geographical distribution, the modified RTS-79 system could be assumed to be entirely located within either section I, II, III or IV. The varying reliability indices results indicate that, for systems with DTR enforced, the neglect of multi-area weather conditions could lead to biased system reliability assessment. In the simulated case, the biases could be up to 7% in the EENS index. Such biases could sometimes be vital for system operators faced with simultaneous component outages. Especially for the proposed DTR-NTO in this study, such biases may lead to false network reconfiguration solutions and bring risks to the system security.

TABLE III
IMPACTS OF MULTI-AREA WEATHER CONDITIONS ON DTR ENFORCED SYSTEM RELIABILITY

System	Cases	LOLE (h/yr.)	EENS (MWh)
Sectionalized RTS-79, 60% transmission capability	Basic OPF	1206.69	205,857
	DTR-OPF, considered multi-area	873.10	147,306
	DTR-OPF, based on Sec. I	795.66	136,966
	DTR-OPF, based on Sec. II	801.23	139,328
	DTR-OPF, based on Sec. III	866.88	147,509
	DTR-OPF, based on Sec. IV	857.39	147,053

B. Performance Comparison of OTS, BBS, and NTO

To demonstrate the performance of NTO and compare it with OTS and BBS, case studies are conducted on the IEEE RTS-79 system with OHLs' rating being modified to 60% of their original values in [49].

TABLE IV
PERFORMANCE COMPARISON OF OPF, OTS, BBS AND NTO

System	Scenarios	LOLE (h/yr.)	EENS (MWh/yr.)
RTS-79, 50% transmission capability	OPF	1092.95	183,656
	OTS	910.05	171,306
	BBS	927.71	172,244
	NTO	908.50	171,287

ation information: DOI 10.1109/TPWRS.2018.2829079, IEEE

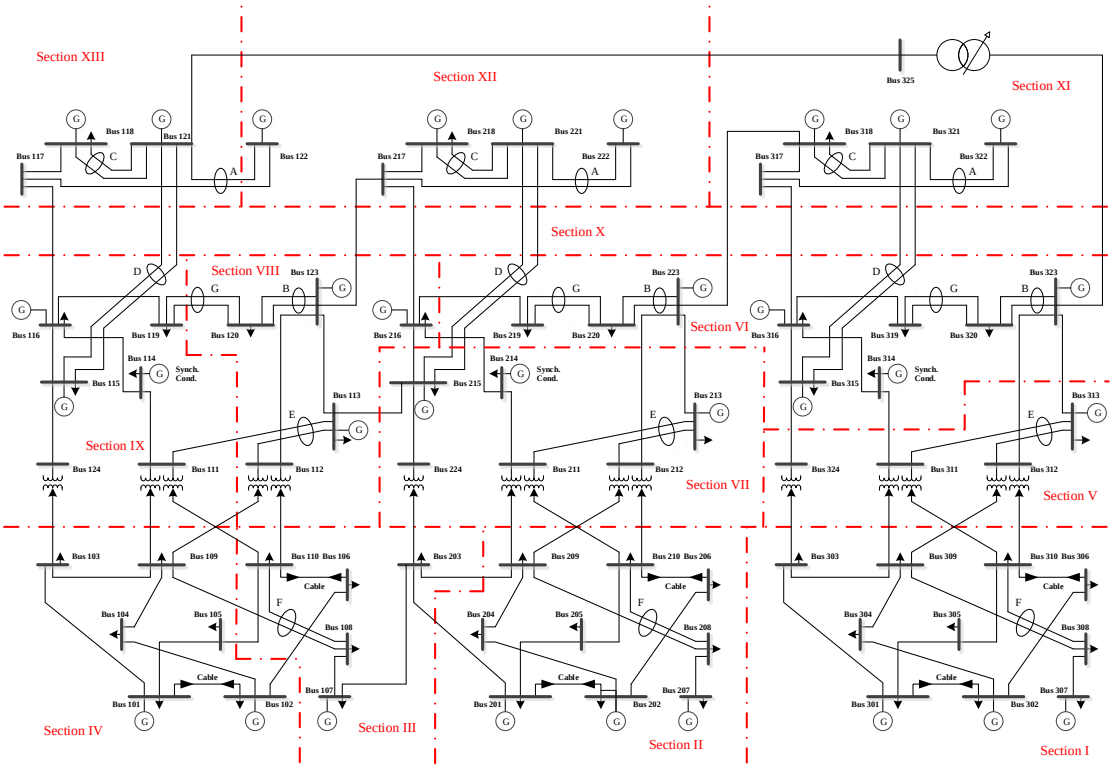

Fig. 8. Sectionalized RTS-96 system reflecting multi-area weather conditions

Table IV lists the system reliability indices with OPF, OTS, BBS and NTO enforcement. The results indicate that, with either OTS, BBS or NTO enforced in the system, the reliability indices will decrease: compared to the basic OPF case, the LOLE index of OTS, BBS and NTO cases has dropped by 16.73%, 18.16%, and 19.88%, respectively; the EENS index of OTS, BBS and NTO cases has dropped by 6.72%, 6.66%, and 7.18%, respectively. Clearly, with the deployment of any of these network topology control technologies, the system reliability could be remarkably enhanced. Yet among all technologies, NTO exhibits a salient reliability reinforcement capability.

In Fig. 9, the average switching actions in each scenario are illustrated. The results indicate that, with the goal of minimizing the system total load curtailment, basically different network topology control techniques require different numbers of switching actions. Specifically, compared to OTS and BBS, the NTO requires fewer average number of line switching actions than OTS, and fewer average number of busbar switching actions than BBS as well. Therefore, the superiority of NTO can be summarized as follows: generally, the NTO offers the system operator with a broader choice of transmission network reconfiguration solutions; with a fewer number of line/busbar switching actions required, a more evident system reliability enhancement may be obtained.

C. Power System Reliability Evaluation Incorporating DTR-NTO

Then to demonstrate the effectiveness of the proposed DTR-NTO methodology, the simulation has been conducted on the sectionalized RTS-79 system with the thermal ratings of all OHLs being modified to be 60% of their original values in [49].

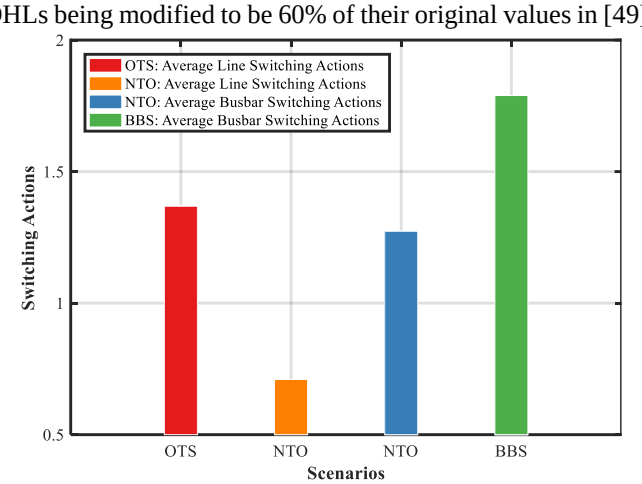

Fig. 9. Average switching actions in each scenario

Based on the proposed methodology presented in section IV, the LOLE and EENS indices obtained are shown in Table V. It is obvious that the incorporation of DTR-NTO results in a significant improvement to the power system reliability: compared with OPF, the LOLE index in DTR-NTO has dropped by 43.84% and the EENS index in DTR-NTO has declined by 38.70%.

TABLE V
MODIFIED RTS-79 SYSTEM RELIABILITY ASSESSMENT RESULTS

System	Scenarios	LOLE (h/yr.)	EENS (MWh/yr.)
Sectionalized RTS-79, 60% transmission capability	OPF	1204.22	210,061
	NTO	1011.68	196,945
	DTR-OPF	853.48	152,174
	DTR-NTO	830.02	151,168

ation information: DOI 10.1109/TPWRS.2018.2829079, IEEE

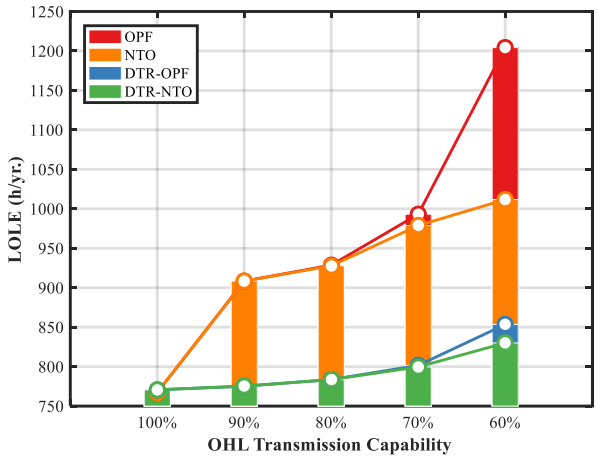

Fig. 10. Modified RTS-79: LOLE with respect to different OHL transmission capabilities

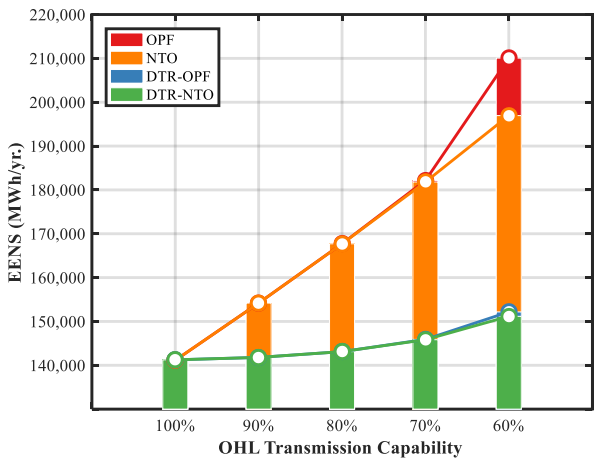

Fig. 11. Modified RTS-79: EENS with respect to different OHL transmission capabilities

Simulations have also been conducted on the sectionalized RTS-79 system with different OHL transmission capabilities. As shown in Fig. 10 and Fig. 11, with the transmission capabilities decreasing from 100% to 60%, both the LOLE and EEND indices increase accordingly. Among all four scenarios, the increase of LOLE and EENS in DTR-NTO scenario remains the smallest: 7.71% and 7.03% compared to 56.94% and 48.83% in OPF. In addition, compared with the other three scenarios, the LOLE and EENS values are also the smallest, inter alia for systems with low transmission capabilities. This observation indicates that the integration of DTR-NTO could help to enhance the power systems reliability. For power grids with aging OHLs or low power delivery capability, the benefits brought by DTR-NTO can be even greater.

To further demonstrate the scalability of the proposed methods and to show the impact of geographical weather variances, more simulations are conducted on the sectionalized RTS-96 system with all OHL transmission capacities being assumed to vary from 100% to 60% of their original values in [50].

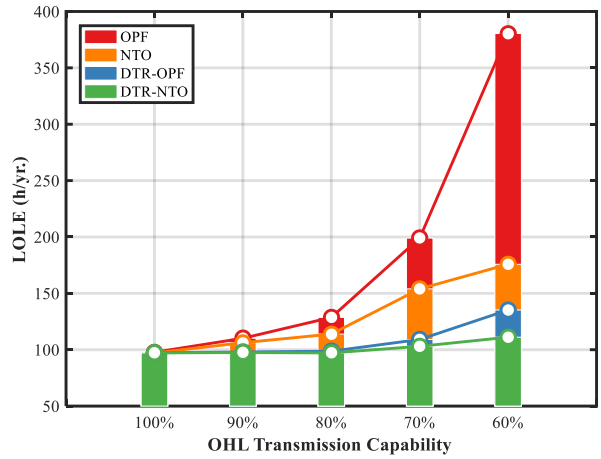

Fig. 12. Modified RTS-96: LOLE with respect to different OHL transmission capabilities

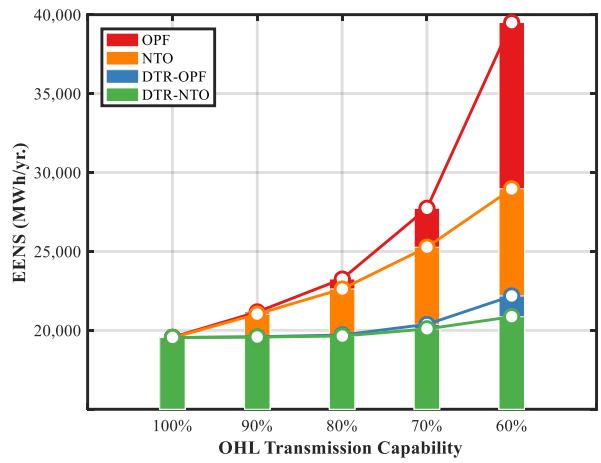

Fig. 13. Modified RTS-96: EENS with respect to different OHL transmission capabilities

The obtained LOLE and EENS indices are illustrated in Fig. 12 and Fig. 13, respectively. As expected, with the enforcement of DTR-NTO the system reliability is dramatically improved: among all four scenarios, the increases of LOLE and EENS in the DTR-NTO scenario are only 14.32% and 6.74%, compared to 289.16% and 101.95% in the OPF scenario. Moreover, the reliability indices in the DTR-NTO scenario are still the smallest among all four test scenarios. Although the enforcement of DTR or NTO alone could help enhance the system reliability already, the enforcement of the proposed joint deployment scheme, namely DTR-NTO, could lead to an even better performance.

Besides the system level performance, particularly the performance of DTR-NTO in some typical sampled system states are demonstrated in Table VI. These sampled system states all consist of severe contingencies: several generation unit outages, and even transmission line outages. With only traditional operating strategies, a great amount of load demands will be curtailed. Yet with DTR, NTO or the DTR-NTO, such load curtailment could be reduced, to a certain extent.

 ation information: DOI 10.1109/TPWRS.2018.2829079, IEEE

TABLE VI
PERFORMANCE COMPARISON IN DIFFERENT SCENARIOS TESTED ON MODIFIED RTS-96

Example States	No. of OHL Outages	No. of Generation Unit Outages	Failed Components	System Load Curtailment (MW)			
				OPF	NTO	DTR-OPF	DTR-NTO
i	1	6	A32-2 G101-4 G118 G121 G123-3 G202-3 G323-3	260.01	57	16.41	0
ii	1	7	CA-1 G102-2 G113-1 G116 G118 G121 G122-2 G322-6	244.3	137	113.77	0
iii	0	10	G102-1 G118 G201-1 G202-2 G301-1 G302-2 G313-3 G321 G323-1 G323-3	156.11	57	102.72	0
iv	0	6	G107-3 G115-4 G118 G121 G318 G323-3	118.95	67	9.63	0
v	0	6	G113-3 G118 G121 G223-1 G321 G322-3	94.15	7	73.95	0
vi	0	5	G121 G218 G221 G223-2 G323-3	113.03	110	54.56	40
vii	0	7	G113-3 G115-6 G116 G123-3 G318 G321 G322-3	155.66	112	59.19	42
viii	0	6	G118 G123-3 G313-2 G315-6 G321 G323-2	123.07	62	101.24	31.06
ix	1	8	A25-1 G101-2 G113-1 G218 G222-5 G301-2 G313-3 G318 G321	100.15	89	80.22	72.73
x	1	8	A25-1 G101-2 G113-1 G218 G222-5 G301-2 G313-3 G318 G321	100.15	89	64.13	39.41

For instance, for the example state iv, load curtailment in the DTR-OPF scenario is reduced to 9.63 MW. Furthermore, in the DTR-NTO scenario load curtailment is reduced to zero. Such results indicate that even with increased dynamic ratings of OHLs, the NTO mechanism may be able to find network reconfiguration solutions which could further reduce the load curtailment. For states ix and x where the failed components are identical, DTR-NTO produces different load curtailment results. Apparently, such results indicate that the weather condition in the time of state x becomes better, which results in further increased OHL dynamic ratings with respect to those in state ix. In such a case, DTR-NTO could find an improved network reconfiguration strategy and help further reduce the load curtailment.

Certainly, the enforcement of DTR-NTO cannot always guarantee a full elimination of load curtailing due to component failures, as shown in sample states vi - x. However, the results imply that the enforcement of DTR-NTO is able to significantly mitigate the load curtailment of highly deficient system states, i.e., those states with severe failures caused by multiple components outages. In sum, the incorporation of DTR-NTO in the operating strategy could help improve the system reliability substantially.

VI. CONCLUSIONS AND FUTURE WORK

This study has incorporated the DTR and NTO mechanisms into the reliability assessment of power system. The impact of multi-area weather conditions on DTR performance has been theoretically discussed and illustrated in simulation. And the different network topology control techniques, the OTS, BBS and NTO has been discussed and compared both in the problem modeling and the practical influence on system reliability.

Simulations have been carried out on the modified IEEE RTS-79 and RTS-96 systems with geographical information reflecting different climatic characteristics. The numerical results obtained indicate that:

1) The consideration of multi-area weather conditions is important in OHL dynamic thermal rating calculations. Neglecting such impacts could lead to biased estimations of DTR performance, and hence bring risks to the system security.
2) The NTO technology which combines line switching and busbar splitting performs better than the traditional network topology control methods. With only a reasonable number of switching actions, NTO could help dramatically improve the system reliability.
3) The joint deployment of DTR-NTO could substantially improve the power system reliability. Such reliability enhancement could be much more significant than the cases where only DTR or NTO is enforced. Particularly, for electricity grids with limited transmission capacities, enforcement of DTR-NTO could become even more beneficial.

For the future work, the impact of renewable energy sources integrations will be investigated based on the proposed method. In addition, the effectiveness of DTR-NTO as remedial operation actions in the face of natural calamities (e.g., hurricanes, earthquakes or snowstorms) and man-made disasters (e.g., major cyberattacks or terrorist attacks) will be studied from the perspective of cyber-physical system resiliency.

REFERENCES

[1] Y. Ding, C. Singh, L. Goel, J. Østergaard, and P. Wang, "Short-Term and Medium-Term Reliability Evaluation for Power Systems with High Penetration of Wind Power," *IEEE Transactions on Sustainable Energy*, vol. 5, no. 3, pp. 896-906, July 2014.

[2] M. Liu, W. Li, C. Wang, R. Billinton and J. Yu, "Reliability Evaluation of a Tidal Power Generation System Considering Tidal Current Speeds," *IEEE Transactions on Power Systems*, vol. 31, no. 4, pp. 3179-3188, July 2016.

[3] L. H. Koh, P. Wang, F. H. Choo, K. J. Tseng, Z. Gao, and H. B. Püttgen, "Operational Adequacy Studies of a PV-Based and Energy Storage

 ation information: DOI 10.1109/TPWRS.2018.2829079, IEEE

Stand-Alone Microgrid," *IEEE Transactions on Power Systems*, vol. 30, no. 2, pp. 892-900, March 2015.

[4] X. Zhang, K. Tomsovic and A. Dimitrovski, "Security Constrained Multi-Stage Transmission Expansion Planning Considering a Continuously Variable Series Reactor," *IEEE Transactions on Power Systems*, vol. 32, no. 6, pp. 4442-4450, Nov. 2017.

[5] X. Zhang, D. Shi, Z. Wang, J Huang, X. Wang, G. Liu and K. Tomsovic, "Optimal Allocation of Static Var Compensator via Mixed Integer Conic Programming," in *IEEE Power & Energy Society General Meeting*, Chicago, IL, 2017, pp. 1-5.

[6] Y. Xu and C. Singh, "Power System Reliability Impact of Energy Storage Integration with Intelligent Operation Strategy," *IEEE Transactions on Smart Grid*, vol. 5, no. 2, pp. 1129-1137, March 2014.

[7] B. Falahati and Y. Fu, "Reliability Assessment of Smart Grids Considering Indirect Cyber-Power Interdependencies," *IEEE Transactions on Smart Grid*, vol. 5, no. 4, pp. 1677-1685, July 2014.

[8] Y. Xiang, Z. Ding, Y. Zhang and L. Wang, "Power System Reliability Evaluation Considering Load Redistribution Attacks," *IEEE Transactions on Smart Grid*, vol. 8, no. 2, pp. 889-901, March 2017.

[9] "Increased Power Flow Guidebook: Increasing Power Flow in Transmission and Substation Circuits," EPRI, Palo Alto, CA, USA, Rep. no. 1010627, Nov. 16, 2005.

[10] M. Heidarifar and H. Ghasemi, "A Network Topology Optimization Model Based on Substation and Node-Breaker Modeling," *IEEE Transactions on Power Systems*, vol. 31, no. 1, pp. 247-255, Jan. 2016

[11] T. Goodwin and C. Smith, "Smart Grid Demonstration Project–Dynamic Line Rating (DLR)–Oncor Electric Delivery," ERCOT Region Operations Training Seminar, TX, USA, 2011.

[12] D. A. Douglass, A. Edris, and G. A. Pritchard, "Field application of a dynamic thermal circuit rating method," *IEEE Transactions on Power Delivery*, vol. 12, no. 2, pp. 823-831, Apr. 1997.

[13] J. Ausen, B. F. Fitzgerald, E. A. Gust, D. C. Lawry, J. P. Lazar, and R. L. Oye, "Dynamic Thermal Rating System Relieves Transmission Constraint," in *Esmo 2006 - 2006 IEEE International Conference on Transmission & Distribution Construction, Operation and Live-Line Maintenance*, Albuquerque, NM, 2006.

[14] M. Khaki, P. Musilek, J. Heckenbergerova, and D. Koval, "Electric power system cost/loss optimization using Dynamic Thermal Rating and linear programming," in *2010 IEEE Electrical Power & Energy Conference*, Halifax, NS, 2010, pp. 1-6.

[15] M. Mahmoudian Esfahani and G. R. Yousefi, "Real Time Congestion Management in Power Systems Considering Quasi-Dynamic Thermal Rating and Congestion Clearing Time," *IEEE Transactions on Industrial Informatics*, vol. 12, no. 2, pp. 745-754, Apr. 2016.

[16] M. Nick, O. Alizadeh-Mousavi, R. Cherkaoui, and M. Paolone, "Security Constrained Unit Commitment with Dynamic Thermal Line Rating," *IEEE Transactions on Power Systems*, vol. 31, no. 3, pp. 2014-2025, May 2016.

[17] C. J. Wallnerstrom, Y. Huang, and L. Soder, "Impact from Dynamic Line Rating on Wind Power Integration," *IEEE Transactions on Smart Grid*, vol. 6, no. 1, pp. 343-350, Jan. 2015.

[18] D. M. Greenwood and P. C. Taylor, "Investigating the Impact of Real-Time Thermal Ratings on Power Network Reliability," *IEEE Transactions on Power Systems*, vol. 29, no. 5, pp. 2460-2468, Sep. 2014.

[19] J. Teh and I. Cotton, "Reliability Impact of Dynamic Thermal Rating System in Wind Power Integrated Network," *IEEE Transactions on Reliability*, vol. 65, no. 2, pp. 1081-1089, Jun. 2016.

[20] K. Kopsidas, A. Kapetanaki, and V. Levi, "Optimal Demand Response Scheduling with Real Time Thermal Ratings of Overhead Lines for Improved Network Reliability," *IEEE Transactions on Smart Grid*, vol. 8, no. 6, pp. 2813-2825, Nov. 2017.

[21] R. Xiao, Y. Xiang, L. Wang, and K. Xie, "Bulk power system reliability evaluation considering optimal transmission switching and dynamic line thermal rating," in *2016 IEEE International Conference on Probabilistic Methods Applied to Power Systems (PMAPS)*, Beijing, 2016, pp. 1-5.

[22] R. P. O'Neill, R. Baldick, U. Helman, M. H. Rothkopf, and W. Stewart Jr, "Dispatchable Transmission in RTO Markets," *IEEE Transactions on Power Systems*, vol. 20, no. 1, pp. 171-179, Feb. 2005.

[23] E. B. Fisher, R. P. O'Neill, and M. C. Ferris, "Optimal Transmission Switching," *IEEE Transactions on Power Systems*, vol. 23, no. 3, pp. 1346-1355, Aug. 2008.

[24] G. Schnyder and H. Glavitsch, "Security enhancement using an optimal switching power flow," *IEEE Transactions on Power Systems*, vol. 5, no. 2, pp. 674-681, May. 1990.

[25] K. W. Hedman, R. P. O'Neill, E. B. Fisher, and S. S. Oren, "Optimal transmission switching with contingency analysis," *IEEE Transactions on Power Systems*, vol. 24, no. 3, pp. 1577-1586, Aug. 2009.

[26] J. Wu and K. W. Cheung, "Incorporating Optimal Transmission Switching in Day-Ahead Unit Commitment and scheduling," in *IEEE Power & Energy Society General Meeting*, Denver, CO, 2015, pp. 1-5.

[27] A. Mazi, B. F. Wollenberg, and M. H. Hesse, "Corrective Control of Power System Flows by Line and Bus-Bar Switching," *IEEE Power Engineering Review*, vol. PER-6, no. 8, pp. 53-53, Aug. 1986.

[28] S. Wei and V. Vittal, "Corrective switching algorithm for relieving overloads and voltage violations," *IEEE Transactions on Power Systems*, vol. 20, no. 4, pp. 1877-1885, Nov. 2005.

[29] R. Billinton and W. Li, "Composite System Adequacy Assessment," in *Reliability Assessment of Electric Power Systems Using Monte Carlo Methods*, 1st ed. New York: Springer US, 1994, ch. 5, pp. 131-144.

[30] C. Tumelo-Chakonta and K. Kopsidas, "Assessing the value of employing dynamic thermal rating on system-wide performance," in *2011 2nd IEEE PES International Conference and Exhibition on Innovative Smart Grid Technologies*, Manchester, 2011, pp. 1-8.

[31] C. R. Black and W. A. Chisholm, "Key Considerations for the Selection of Dynamic Thermal Line Rating Systems," *IEEE Transactions on Power Delivery*, vol. 30, no. 5, pp. 2154-2162, Oct. 2015.

[32] F. Qiu and J. Wang, "Distributionally Robust Congestion Management with Dynamic Line Ratings," *IEEE Transactions on Power Systems*, vol. 30, no. 4, pp. 2198-2199, July 2015.

[33] J. Teh and I. Cotton, "Critical span identification model for dynamic thermal rating system placement," *IET Generation, Transmission & Distribution*, vol. 9, no. 16, pp. 2644-2652, Dec. 2015.

[34] D. Roberts, P. Taylor and A. Michiorri, "Dynamic thermal rating for increasing network capacity and delaying network reinforcements," in *CIRED Seminar 2008: SmartGrids for Distribution*, Frankfurt, 2008, pp. 1-4.

[35] P. Pramayon, S. Guerard, G. Aanhaanen, B. Kresimir, P. Cachtpole, M. Norton, R. Puffer, A. Sorensen, M. Weibel, G. Brennan, J. Rogier, P. Southwell, and B. Wareing, "Increasing Capacity of Overhead Transmission Lines - Needs and Solutions," CIGRE Working Group B2/C1.19, Paris, France, Technical Brochure 425, 2011.

[36] M. W. Davis, "A new thermal rating approach: The real time thermal rating system for strategic overhead conductor transmission lines -- Part I: General description and justification of the real time thermal rating system," *IEEE Transactions on Power Apparatus and Systems*, vol. 96, no. 3, pp. 803-809, May 1977.

[37] *IEEE Standard for Calculating the Current-Temperature Relationship of Bare Overhead Conductors*, IEEE Std 738-2012 (Revision of IEEE Std 738-2006 - Incorporates IEEE Std 738-2012 Cor 1-2013), 23 Dec. 2013.

[38] *Overhead Electrical Conductors - Calculation Methods for Stranded Bare Conductors*, IEC/TR 61597-1995, 05 May. 1995.

[39] *Guide for Thermal Rating Calculation of Overhead Lines*, CIGRE Technical brochure 601, Dec. 2014.

[40] Ł. Staszewski and W. Rebizant, "Avoiding blackouts with dynamic thermal line rating," in *2015 Modern Electric Power Systems (MEPS)*, Wroclaw, 2015, pp. 1-5.

[41] Arroyo, P. Castro, R. Martinez, M. Manana, A. Madrazo, R. Lecuna, and A. Gonzalez, "Comparison between IEEE and CIGRE Thermal Behaviour Standards and Measured Temperature on a 132-kV Overhead Power Line," *Energies*, vol. 8, no. 12, pp. 13660-13671, Dec. 2015.

[42] N. P. Schmidt, "Comparison between IEEE and CIGRE ampacity standards," *IEEE Transactions on Power Delivery*, vol. 14, no. 4, pp. 1555-1559, Oct. 1999.

[43] D. M. Greenwood, J. P. Gentle, K. S. Myers, P. J. Davison, I. J. West, J. W. Bush, G. L. Ingram, and M. C. M. Troffaes, "A Comparison of Real-Time Thermal Rating Systems in the U.S. and the U.K," *IEEE Transactions on Power Delivery*, vol. 29, no. 4, pp. 1849-1858, Aug. 2014.

[44] H. Banakar, N. Alguacil, and F. D. Galiana, "Electrothermal coordination part I: theory and implementation schemes," *IEEE Transactions on Power Systems*, vol. 20, no. 2, pp. 798-805, May 2005.

[45] V. Cecchi, A. S. Leger, K. Miu and C. O. Nwankpa, "Incorporating Temperature Variations into Transmission-Line Models," *IEEE Transactions on Power Delivery*, vol. 26, no. 4, pp. 2189-2196, Oct. 2011.

[46] V. Cecchi, M. Knudson and K. Miu, "System Impacts of Temperature-Dependent Transmission Line Models," *IEEE Transactions on Power Delivery*, vol. 28, no. 4, pp. 2300-2308, Oct. 2013.

[47] ISO New England, *Transmission Owners and ISO-NE Substation Bus*

ation information: DOI 10.1109/TPWRS.2018.2829079, IEEE

Arrangement Guideline Working Group Report, 2006.

[48] IBM. (2016). *IBM ILOG CPLEX V12.6*. [Online]. Available: http://www.ibm.com/support/knowledgecenter/SSSA5P_12.6.0/ilog.odms.cplex.help/CPLEX/homepages/CPLEX.html

[49] P. M. Subcommittee, "IEEE reliability test system," *IEEE Transactions on Power Apparatus and Systems*, vol. PAS-98, no. 6, pp. 2047-2054, Nov. 1979.

[50] C. Grigg, P. Wong, P. Albrecht, R. Allan, M. Bhavaraju, R. Billinton, Q. Chen, C. Fong, S. Haddad, S. Kuruganty, W. Li, R. Mukerji, D. Patton, N. Rau, D. Reppen, A. Schneider, M. Shahidehpour, and C. Singh, "The IEEE reliability test system-1996. A report prepared by the reliability test system task force of the application of probability methods subcommittee," *IEEE Transactions on Power Systems*, vol. 14, no. 3, pp. 1010-1020, Aug. 1999.

[51] Arguez, I. Durre, S. Applequist, M. Squires, R. Vose, X. Yin, and R. Bilotta. (2010). *NOAA's US climate normals (1981–2010)*. [Online]. Available: https://www.ncdc.noaa.gov/cdo-web/datatools/normals